Solution and Performance Analysis of Geolocation by TDOA

K. C. HO
Y. T. CHAN
Royal Military College of Canada

One method of geolocation is based on measuring the time difference of arrivals (TDOAs) of a signal received by three or four geostationary satellites. The received signals are cross-correlated to determine the TDOAs and a set of nonlinear equations are solved to produce the location estimate. An exact solution for the transmitter position is derived for the three or four receiver cases. Extension of the solution method to more receivers is straightforward. An analysis of the performance of the system is given, together with expressions for predicting the localization mean-square error (MSE) and bias, and the Cramér-Rao bound. Both precision in TDOA measurements and the relative geometry between receivers and transmitter affect the localization accuracy. The geometric factors act as multipliers to the TDOA variance in the bias and MSE formulae. A study of the dependency of the geometric factors on transmitter position and satellite spacings are provided, as well as simulation results.

Manuscript received November 27, 1992.
IEEE Log No. T-AES/29/4/10998.

I. INTRODUCTION

Geolocation of a radio transmitter has a wide variety of applications. One example is in locating an emergency radio source for ship or plane rescue [1]. Another is in finding the position of an interference source which interferes with satellite operations [2].

Geolocation is based on techniques which rely on one or a combination of frequency, time and spatial information. Existing methodologies are the differential Doppler (DD) and time difference of arrivals (TDOA) techniques. The DD method uses lower orbit satellites to do a series of DD measurements for localization. Since it is based on frequency shift, the signal should be narrowband, preferably a pure sinusoid. This technique has been adopted in the search and rescue satellite (SARSAT) localization system [1]. Although a minimum of one satellite is sufficient, it takes two passes for localization and the response time is typically up to two hours. The delay can be reduced by using more than one satellite. In the TDOA approach, a minimum of three satellites are required for unambiguous positioning. With three receivers of known positions, the two TDOAs of a signal received by satellites define two hyperboloids in which the transmitter must lie. If the source is on Earth, the intersection of the two curves on the Earth surface defines the transmitter position. TDOA method can locate a wide range of signal types, which makes it attractive for passive localization.

Geolocation via geostationary satellites has received much attention recently [2–4]. The system cost is little as we can make use of many existing satellites. There is no need to launch extra satellites especially for geolocation purposes. In addition, geostationary satellites are motionless with respect to a point on the Earth. This allows accurate TDOA measurements to reduce error. Finally, they are in high altitude and cover a large area on Earth. The response time for localization can be very short.

Geolocation using geostationary satellites from TDOA measurements is studied and analyzed here. Section II is a description of the system. After measuring the TDOAs, it is necessary to solve a set of nonlinear equations to obtain the transmitter location. This is not an easy task and previous work relies on iterative method and linearization [5, 6]. This is computationally expensive and requires an initial guess close to the true solution, which may not be easy to select in practice. Although [7] has derived solutions for hyperbolic fixes, it is not applicable to an overdetermined situation in which more TDOAs are available to reduce error. We propose a new solution in Section II. The solution is exact and eliminates the problems associated with existing iterative techniques. In addition, it can be easily extended to overdetermined situations. Position accuracy is of great concern in localization. The study by Chestnut [8] is

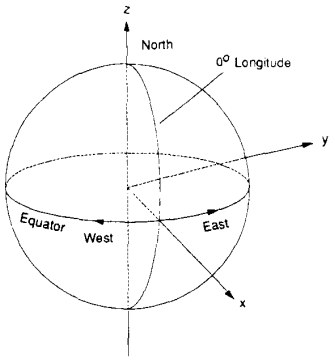

Fig. 1. Geocentric coordinate system.

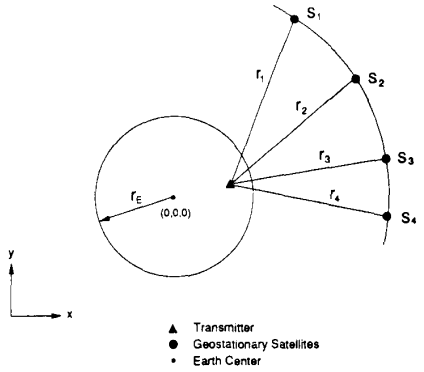

Fig. 2. Geolocation by geostationary satellite.

incomplete as only one sigma error of a single TDOA curve on the Earth surface is provided. Sonnenschein and Hutchison [4] simply adds the error squared of the two TDOA curves to form the location MSE by assuming the two TDOA curves independent. The correlation between the two curves are not taken into account. The position variance from Torrieri [6] is for iterative solution only, not for exact solution. We provide in Section III a precise evaluation and analysis of the system. In particular, the mean-square error (MSE) and bias formulae are derived. Section IV presents simulation results to support and corroborate the theoretical developments. Conclusions are given in Section V.

II. TDOA GEOLOCATION WITH GEOSTATIONARY SATELLITES

The geocentric coordinate system is commonly adopted in geolocation. As shown in Fig. 1, the x axis is the intersection of the equatorial plane and the Greenwich meridian plane and is oriented from the center of the Earth, the z axis is the axis of the rotation of the Earth, and the y axis completes the right-handed Cartesian coordinate system. The orbit that geostationary satellites occupy is a circle of radius r_s approximately 42164 km lying in the equatorial plane.

TDOA measures the difference in arrival times of a signal at two separate locations. Typically, the measurement consists of prefiltering and then cross-correlating the outputs of receivers [9]. The time from origin at which the correlation function attains the largest value is taken as the TDOA. When there are more than two receivers, we have several TDOA measurements. Hahn and Tretter [10] have proposed to process the set of TDOAs to increase accuracy. The method comprises of measuring TDOAs for all possible receiver pairs via cross-correlation and then using the Gauss-Markov estimate of the TDOA values with respect to the first receiver as the final result. It has been proved that this method can achieve the Cramér-Rao lower bound (CRLB) and the final TDOA estimates satisfy the relation

$$D_{i,j} = D_{i,k} - D_{k,j} \tag{1}$$

where $D_{i,j}$ is the TDOA between receivers i and j. It is shown in Appendix A that the TDOA for geostationary satellite receivers cannot exceed 19.64 ms. Maximum TDOA occurs when a transmitter is on the equator with its longitude equal to that of one of the satellites, while the other is 81.3° apart.

In practice, only a limited number of receivers are available. A minimum of three satellites are needed when the transmitter is known to be on the Earth surface and four if the altitude of the transmitter is not known. Let s_i, $i = 1,2,3,4$, be the geostationary satellites. Referring to Fig. 2, let $D_{i+1,i}$, $i = 1,2,3$, be the TDOA measured between s_{i+1} and s_i. If c is the signal propagation speed, then

$$r_{i+1,i} = cD_{i+1,i} = r_{i+1} - r_i, \qquad i = 1,2,3 \tag{2}$$

with r_i denoting the distance between the transmitter and the ith satellite. Let s_i be at a known position (x_i, y_i, z_i), $i = 1,2,3,4$ and the transmitter unknown coordinates be (x,y,z), then

$$r_i^2 = (x_i - x)^2 + (y_i - y)^2 + (z_i - z)^2,$$

$$i = 1,2,3,4. \tag{3}$$

Solving (2)–(3) gives the emitter position. This is not an easy task because the equations involved are nonlinear. Iterative solution by linearization using Taylor series expansion is one way [5, 6]. It requires a proper initial position guess close to the true solution and convergence is not guaranteed. The result for position fix in [7] is not in the geocentric coordinate system and proper coordinate transformation is required. In addition, it can only be applied to critically determined situation. We provide another solution method.

Consider first the three receiver case. Denote r_E as the Earth radius (6378 km). Since the transmitter is on Earth, its coordinates must satisfy

$$r_E^2 = x^2 + y^2 + z^2. \tag{4}$$

Let K_i be $x_i^2 + y_i^2 + z_i^2$. Equation (3) can be rewritten as

$$2x_i x + 2y_i y + 2z_i z = K_i + r_E^2 - r_i^2, \quad i = 1,2,3. \tag{5}$$

From (2), we have

$$r_{i+1}^2 = (r_i + r_{i+1,i})^2 = r_i^2 + 2r_{i+1,i}r_i + r_{i+1,i}^2, \quad i = 1,2. \tag{6}$$

Hence

$$\begin{bmatrix} x_1 & y_1 & z_1 \\ x_2 & y_2 & z_2 \\ x_3 & y_3 & z_3 \end{bmatrix} \begin{bmatrix} x \\ y \\ z \end{bmatrix} = \frac{1}{2} \begin{bmatrix} K_1 + r_E^2 + r_{2,1}^2 + 2r_{2,1}r_2 - r_2^2 \\ K_2 + r_E^2 - r_2^2 \\ K_3 + r_E^2 - r_{3,2}^2 - 2r_{3,2}r_2 - r_2^2 \end{bmatrix}. \tag{7}$$

By inverting the matrix formed by satellite positions, we can express the transmitter coordinates in terms of r_2. Substitution of this result into (3) with $i = 2$ produces a 4th-order equation for r_2, which can then be solved. Inserting the positive r_2 values into (7) gives at most four possible transmitter positions. The proper solution is obtained from knowing in which quadrant the transmitter lies.

In the four receiver case, we observe that from (1),

$$\begin{cases} r_{3,2} + r_{2,1} - r_{3,1} = 0 \\ r_{4,3} + r_{3,1} - r_{4,1} = 0 \\ r_{4,2} + r_{2,1} - r_{4,1} = 0 \\ r_{4,3} + r_{3,2} - r_{4,2} = 0 \end{cases}. \tag{8}$$

Using the relation $r_{i,j} = r_i - r_j$, we have

$$r_{3,2}r_{2,1}r_{3,1} = r_{3,2}r_1^2 + r_{2,1}r_3^2 - r_{3,1}r_2^2. \tag{9}$$

When (3) is substituted and (8) is used, (9) can be expressed as a linear equation in (x,y,z):

$$r_{3,2}r_{2,1}r_{3,1} = l_1 + m_1 x + u_1 y + v_1 z \tag{10}$$

with

$$l_1 = r_{3,2}K_1 + r_{2,1}K_3 - r_{3,1}K_2$$

$$m_1 = -2(r_{3,2}x_1 + r_{2,1}x_3 - r_{3,1}x_2)$$

$$u_1 = -2(r_{3,2}y_1 + r_{2,1}y_3 - r_{3,1}y_2)$$

$$v_1 = -2(r_{3,2}z_1 + r_{2,1}z_3 - r_{3,1}z_2).$$

Similarly,

$$r_{4,3}r_{3,1}r_{4,1} = r_{4,3}r_1^2 + r_{3,1}r_4^2 - r_{4,1}r_3^2 = l_2 + m_2 x + u_2 y + v_2 z \tag{11}$$

$$r_{4,2}r_{2,1}r_{4,1} = r_{4,2}r_1^2 + r_{2,1}r_4^2 - r_{4,1}r_2^2 = l_3 + m_3 x + u_3 y + v_3 z \tag{12}$$

$$r_{4,3}r_{3,2}r_{4,2} = r_{4,3}r_2^2 + r_{3,2}r_4^2 - r_{4,2}r_3^2 = l_4 + m_4 x + u_4 y + v_4 z \tag{13}$$

where l_i, m_i, u_i, v_i, $i = 2,3,4$ are defined analogous to those equations below (10). It appears that there are four linear equations in (x,y,z). They are, however, dependent because by using (8), we find (10) + (11) − (12) = (13). Moreover, $r_{4,1}$(10) + $r_{2,1}$(11) = $r_{3,1}$(12). Thus there are only two independent equations. Now, x and y can be determined in terms of z from (10)–(11),

$$\begin{bmatrix} m_1 & u_1 \\ m_2 & u_2 \end{bmatrix} \begin{bmatrix} x \\ y \end{bmatrix} = \begin{bmatrix} r_{3,2}r_{2,1}r_{3,1} - l_1 - v_1 z \\ r_{4,3}r_{3,1}r_{4,1} - l_2 - v_2 z \end{bmatrix}. \tag{14}$$

With (3), the temporary result is substituted into (2) at any one i to form a quadratic equation in z, which can be solved. Inserting the roots into (14) gives 2 solutions. Transmitter position is obtained by knowing the directions in which the receiving antennas are pointed to. We note that the two solutions given here for the three and four satellites are new and are different from those in [3, 5, 6] which require either linearization or iteration.

Our solution method can be easily extended to the situation where extra TDOAs (from extra satellites) are available to reduce the estimation error. The method in [7] cannot incorporate such additional TDOA measurements. In this case, we simply add more rows to (7) and (14) and perform pseudoinversion of the matrics to express the transmitter position in terms of r_2 when the transmitter is on Earth and (x,y) in terms of z when the transmitter altitude is not known. The remaining steps remain the same.

III. GEOLOCATION ACCURACY

There are always uncertainties in TDOA measurements [10] and satellite positions [3]. These inaccuracies give rise to random errors in the emitter location. Although [8] has provided one sigma error of a TDOA curve on the Earth surface, the location accuracy of a transmitter is unavailable. Reference [4] forms the position MSE by adding the error squared of the two TDOA curves, with the assumption that the two curves are statistically independent. But a TDOA estimator, because the same signal is present in all measurements, always generates correlated TDOA

measurements, rendering the assumption invalid and underestimating the true MSE. References [5, 6] have derived the location variance for an iterative solution. The formula is not appropriate in our case as our solution is exact. In addition, the relation between accuracy and the localization geometry is not explicitly shown. We give a precise study of the geolocation accuracy through the quantities of localization MSE and bias. For presentation simplicity, we consider only the three-receiver case where the transmitter is on the Earth surface. The localization accuracy in the four-receiver case can be derived in a similar fashion.

A. Transmitter Location MSE

Denote the true transmitter location as (x^0, y^0, z^0). From the differentials of (2)–(4), and if the error vector $\Delta\mathbf{u} = [\Delta x, \Delta y, \Delta z]^T = [x - x^0, y - y^0, z - z^0]^T$ is small, the errors must satisfy the matrix equation

$$\begin{bmatrix} \underbrace{\frac{x_1 - x^0}{r_1} - \frac{x_2 - x^0}{r_2}}_{x^0} & \underbrace{\frac{y_1 - y^0}{r_1} - \frac{y_2 - y^0}{r_2}}_{y^0} & \underbrace{\frac{z_1 - z^0}{r_1} - \frac{z_2 - z^0}{r_2}}_{z^0} \\ \underbrace{\frac{x_2 - x^0}{r_2} - \frac{x_3 - x^0}{r_3}}_{x^0} & \underbrace{\frac{y_2 - y^0}{r_2} - \frac{y_3 - y^0}{r_3}}_{y^0} & \underbrace{\frac{z_2 - z^0}{r_2} - \frac{z_3 - z^0}{r_3}}_{z^0} \end{bmatrix} \begin{bmatrix} \Delta x \\ \Delta y \\ \Delta z \end{bmatrix} = \begin{bmatrix} c\Delta D_{2,1} \\ c\Delta D_{3,2} \\ 0 \end{bmatrix} \tag{15}$$

where $\Delta D_{i+1,i}$ is the deviation of $D_{i+1,i}$ from their mean values. Denote the matrix in (15) as $\mathbf{G}$ and the vector on the right $\mathbf{h}$. If $\mathbf{G}$ is of full rank, the error vector is given by $\Delta\mathbf{u} = \mathbf{G}^{-1}\mathbf{h}$. Hence the MSE matrix is

$$E[\Delta\mathbf{u}\Delta\mathbf{u}^T] = \mathbf{G}^{-1}\mathbf{E}[\mathbf{h}\mathbf{h}^T]\mathbf{G}^{-T}. \tag{16}$$

Given the TDOA covariance matrix and coordinates of the transmitter and receivers, the error matrix can be evaluated. The position MSE is then equal to the trace of $E[\Delta\mathbf{u}\Delta\mathbf{u}^T]$.

Equation (16) cannot provide much insight on how the MSE is being affected by various factors such as transmitter position, receiver positions, etc. We derive an alternative formula for MSE, which can provide the information about the dependency of MSE on localization configuration and is simpler to evaluate.

In [8], there is a formula for the one-sigma width of a curve of constant TDOA on the Earth surface. The MSE is found based on this result. TDOAs and transmitter position are related to each other by (2)–(3). Expanding (2) in Taylor series about the true transmitter location and ignoring the high order terms gives

$$c\Delta D_{i+1,i} \approx \nabla\mathbf{r}_{i+1,i} \cdot \Delta\mathbf{n}_i + \sum_j \frac{\partial r_{i+1,i}}{\partial p_j}\Delta p_j, \quad i = 1,2 \tag{17}$$

where the symbol $\cdot$ represents dot product, $\nabla\mathbf{r}_{i+1,i}$ is the gradient vector of $r_{i+1,i}$ with respect to x, y and z evaluated at x^0, y^0 and z^0, $\Delta\mathbf{n}_i$ is the component of the error vector $\Delta\mathbf{u}$ that is parallel to $\nabla\mathbf{r}_{i+1,i}$, and Δp_j are variations in satellite positions. $||\Delta\mathbf{n}_i||$ is a measure of the deviations of the hyperbolae defined by (2) incurred by changes in TDOAs, where the symbol $||*||$ designates the Euclidean norm of $*$. Taking absolute value of (17), we have

$$||\Delta\mathbf{n}_i|| = \frac{|c\Delta D_{i+1,i} - \sum_j \frac{\partial r_{i+1,i}}{\partial p_j}\Delta p_j|}{||\nabla\mathbf{r}_{i+1,i}||}, \quad i = 1,2. \tag{18}$$

Fig. 3 illustrates how the transmitter location varies in accordance with changes in the hyperbolae on the Earth surface. The true transmitter position is at t. C_1 and C_2 are the error-free measurement curves with an intersection angle α, $0° \le \alpha < 90°$. $\Delta\mathbf{n}_{1E}$ and $\Delta\mathbf{n}_{2E}$, which come from $\Delta\mathbf{n}_1$, and $\Delta\mathbf{n}_2$, are, respectively, random position vectors of C_1 and C_2. They have magnitudes equal to [8]

$$||\Delta\mathbf{n}_{iE}|| = \frac{||\Delta\mathbf{n}_i||}{\sin\psi_i}, \quad i = 1,2 \tag{19}$$

where ψ_i is the angle between $\nabla\mathbf{r}_{i+1,i}$ and $\mathbf{r}$, and $\mathbf{r}$ is the unit vector from the center of Earth in the direction of the transmitter. Notice that $\Delta\mathbf{n}_{iE}$ is perpendicular to C_i, $\Delta\mathbf{n}_{L1}$ and $\Delta\mathbf{n}_{L2}$ are random error vectors of the transmitter position estimate. The actual location error vector $\Delta\mathbf{n}_L$ is $\Delta\mathbf{n}_{L1}$ if the angle

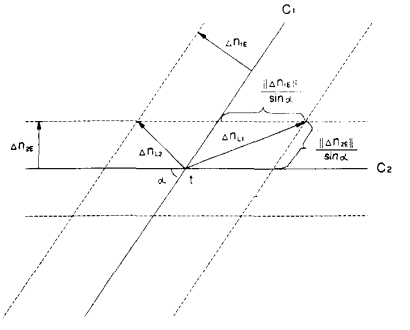

Fig. 3. Variations in location estimate due to uncertainty in hyperbolic curves.

between $\Delta\mathbf{n}_{1E}$ and $\Delta\mathbf{n}_{2E}$ is greater than 90° and is $\Delta\mathbf{n}_{L2}$ otherwise. Thus

$$\begin{aligned}\text{MSE} &= E[\|\Delta\mathbf{n}_L\|^2] \\ &= E[\|\Delta\mathbf{n}_{L1}\|^2 \mid \Delta\mathbf{n}_{1E}\cdot\Delta\mathbf{n}_{2E}<0] \\ &\quad\times \Pr(\Delta\mathbf{n}_{1E}\cdot\Delta\mathbf{n}_{2E}<0) \\ &\quad + E[\|\Delta\mathbf{n}_{L2}\|^2 \mid \Delta\mathbf{n}_{1E}\cdot\Delta\mathbf{n}_{2E}>0] \\ &\quad\times \Pr(\Delta\mathbf{n}_{1E}\cdot\Delta\mathbf{n}_{2E}>0). \end{aligned} \tag{20}$$

Referring to Fig. 3 and using the cosine law, we find

$$\begin{aligned}\|\Delta\mathbf{n}_{Li}\|^2 = \frac{1}{\sin^2\alpha}\{&\|\Delta\mathbf{n}_{1E}\|^2 + \|\Delta\mathbf{n}_{2E}\|^2 \\ &+ (-1)^{i-1}2\cos\alpha\|\Delta\mathbf{n}_{1E}\|\|\Delta\mathbf{n}_{2E}\|\}, \\ & i=1,2. \end{aligned} \tag{21}$$

Hence

$$\begin{aligned}\text{MSE} = \frac{1}{\sin^2\alpha}\{&E[\|\Delta\mathbf{n}_{1E}\|^2] + E[\|\Delta\mathbf{n}_{2E}\|^2] \\ &+ 2\cos\alpha(E[\|\Delta\mathbf{n}_{1E}\|\|\Delta\mathbf{n}_{2E}\| \\ &\quad\times \mid \Delta\mathbf{n}_{1E}\cdot\Delta\mathbf{n}_{2E}<0] \\ &\times \Pr(\Delta\mathbf{n}_{1E}\cdot\Delta\mathbf{n}_{2E}<0) \\ &- E[\|\Delta\mathbf{n}_{1E}\|\|\Delta\mathbf{n}_{2E}\| \mid \Delta\mathbf{n}_{1E}\cdot\Delta\mathbf{n}_{2E}>0] \\ &\times \Pr(\Delta\mathbf{n}_{1E}\cdot\Delta\mathbf{n}_{2E}>0))\}. \end{aligned} \tag{22}$$

Since $\Delta\mathbf{n}_{1E}$ and $\Delta\mathbf{n}_{2E}$ are due to TDOA variations and the two TDOAs $D_{2,1}$ and $D_{3,2}$ are correlated (both of them depend on the output of s_2), $\Pr(\Delta\mathbf{n}_{1E}\cdot\Delta\mathbf{n}_{2E}>0) \neq \Pr(\Delta\mathbf{n}_{1E}\cdot\Delta\mathbf{n}_{2E}<0) \neq 0.5$. In our geolocation problem, the two events $\{\Delta\mathbf{n}_{1E}\cdot\Delta\mathbf{n}_{2E}<0\}$ and $\{\Delta\mathbf{n}_1\cdot\Delta\mathbf{n}_2<0\}$ are equivalent. When the uncertainty in satellite positions are small compared with $cD_{i+1,i}$, we can observe from (17) that $\Delta\mathbf{n}_i$ and $\nabla\mathbf{r}_{i+1,i}$ are in the same direction if $\Delta D_{i+1,i}$ is positive and that the direction of $\Delta\mathbf{n}_i$ changes if the sign of $\Delta D_{i+1,i}$ reverses. It was proved in Appendix B that the angle between $\nabla\mathbf{r}_{2,1}$ and $\nabla\mathbf{r}_{3,2}$ is less than 90°. Consequently, the two events $\{\Delta\mathbf{n}_1\cdot\Delta\mathbf{n}_2<0\}$ and $\{\Delta D_{2,1}\cdot\Delta D_{3,2}<0\}$ are also equivalent and

$$\Pr(\Delta\mathbf{n}_{1E}\cdot\Delta\mathbf{n}_{2E}<0) = \Pr(\Delta D_{2,1}\cdot\Delta D_{3,2}<0). \tag{23}$$

Let the variances of $D_{3,2}$ and $D_{2,1}$ be σ^2_{D32} and σ^2_{D21}, respectively, and let their covariance be $\sigma_{D21,D32}$. If $E[\Delta p_i^2] = \sigma_p^2$ for all i and $E[\Delta p_i\Delta p_j] = 0$ for all $i \neq j$, it follows from (18) and (19) that [8],

$$\begin{aligned}E[\|\Delta\mathbf{n}_{iE}\|^2] &= (c^2\sigma^2_{Di+1,i} + 2\sigma_p^2)w_i^2 \\ w_i &= \{2\sin(\theta_{i+1,i}/2)\sin\psi_i\}^{-1}, \\ & i=1,2. \end{aligned} \tag{24}$$

Since both $\Delta\mathbf{n}_{1E}$ and $\Delta\mathbf{n}_{2E}$ are affected by position variations in s_2,

$$\begin{aligned}&E[\|\Delta\mathbf{n}_{1E}\|\|\Delta\mathbf{n}_{2E}\|\,|\Delta\mathbf{n}_{1E}\cdot\Delta\mathbf{n}_{2E}<0] \\ &\quad\geq (c^2E[|\Delta D_{2,1}\Delta D_{3,2}| \mid \Delta D_{2,1}\cdot\Delta D_{3,2}<0] \\ &\qquad - \sigma_p^2 - m_1 - m_2)w_1w_2 \\ &E[\|\Delta\mathbf{n}_{1E}\|\|\Delta\mathbf{n}_{2E}\|\,|\Delta\mathbf{n}_{1E}\cdot\Delta\mathbf{n}_{2E}>0] \\ &\quad\geq (c^2E[|\Delta D_{2,1}\Delta D_{3,2}| \mid \Delta D_{2,1}\cdot\Delta D_{3,2}>0] \\ &\qquad - \sigma_p^2 - m_1 - m_2)w_1w_2 \end{aligned} \tag{25}$$

where $m_i = E[|\Delta D_{i+1,i}|]\sum_j |\partial r_{i+1,i}/\partial p_j|E[|\Delta p_j|]$, with equality holding when $\sigma_p^2 = 0$. The angle α, which is found in Appendix C, is given by

$$\alpha = \cos^{-1}\frac{\cos(\theta_{3,1}/2) - \cos\psi_1\cos\psi_2}{\sin\psi_1\sin\psi_2} \tag{26}$$

and the angles ψ_i are [8]

$$\psi_i = \cos^{-1}\frac{\cos\phi_i - \cos\phi_{i+1}}{2\sin(\theta_{i+1,i}/2)}, \qquad i=1,2 \tag{27}$$

where $\theta_{i,j}$ is the angle subtended at the transmitter by receivers i and j, ϕ_i is the angle between $\mathbf{r}$ and ρ_i, and ρ_i is the unit vector from the point (x^0, y^0, z^0) to the ith receiver. When the joint probability density function (pdf) of the TDOAs is available, the MSE can be evaluated from (22)–(27) at a particular transmitter location. It is important to point out that the MSE is not only dependent on the variances and joint pdf of TDOAs, but also on the relative geometry between satellites and transmitter.

The MSE is greatly affected by the multiplicative factor $(\sin\alpha)^{-2}$. Obviously, we prefer a large intersection angle. Considering ψ_1 and ψ_2 as variables independent of $\theta_{3,1}$, taking partial derivative of α in (26) shows that it is proportional to $\theta_{3,1}$. Increasing the distance between s_1 and s_3 increases $\theta_{3,1}$ and hence α. Thus it would be better to separate the receivers as large as possible. For a certain altitude, however, there exists a limit on satellite separation, as illustrated in Appendix D. More importantly, to retain high signal-to-noise ratio (SNR) to keep small TDOA variance, satellites should be within the beamwidth of a transmitting antenna, which inevitably restricts how far apart the satellites can be.

In an ideal situation, the z coordinate of satellites is zero. Referring to Fig. 4, a transmitter on the equator makes $\phi_2 = \phi_1 - \theta_{2,1}$ and $\phi_3 = \phi_1 - \theta_{3,1} = \phi_2 - \theta_{3,2}$ (at some other positions on the equator, the relationship among ϕ_1, ϕ_2 and ϕ_3 may be different but we will

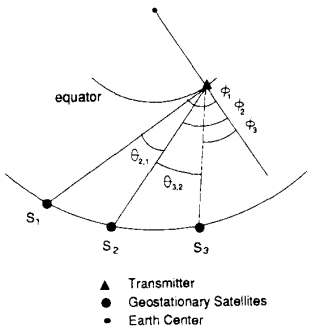

Fig. 4. Relationship between ϕ_i and $\theta_{i+1,i}$ for a transmitter at the equator.

come to the same result below). Using (27) and the sum to product trigonometric identity, we can deduce that $\psi_1 = 90° + (\phi_1 + \phi_2)/2$ and $\psi_2 = 90° + (\phi_2 + \phi_3)/2$. Hence $\psi_1 - \psi_2 = \theta_{3,1}/2$. Using $\sin\psi_1 \sin\psi_2 = \cos(\psi_1 - \psi_2) - \cos\psi_1 \cos\psi_2$ in (26), we find $\alpha = 0$. This implies that the two hyperbolic curves on the Earth are parallel to each other, creating a large uncertainty in position fixing and making the MSE infinite. Although in practice z_i are different from zero, they are very small compared with x_i and y_i and we still have $\alpha \approx 0$. As a result, the equator is the blind region for localization using geostationary satellites. An intuitive explanation for this is that for a transmitter and satellites all on the equatorial plane, the TDOAs do not contain information in the z coordinate. As a result, the z coordinate of the transmitter cannot be determined.

B. Minimum MSE

For simplicity, satellite positions are assumed to be known exactly. We observe from (22)–(25) that the location MSE increases as variance of TDOAs. Minimum TDOA variances correspond to the smallest MSE for a particular localization geometry.

The Cramér-Rao inequality gives a lower bound for the variance of any unbiased parameter estimators. If we assume, for simplicity, that the signal and noises are white of same bandwidth B and that the input SNRs for the three receivers are identical, the CRLB for the TDOAs is [10]

$$\sigma_D^2 = \sigma_{D21}^2 = \sigma_{D32}^2 = \frac{2}{3}\frac{3}{8\pi^2}\frac{1+3\mathrm{SNR}}{\mathrm{SNR}^2}\frac{1}{B^3T}, \qquad (28)$$

$$\sigma_{D21,D32} = -\tfrac{1}{2}\sigma_D^2$$

and T is the observation time. The bound illustrates that increasing SNR, bandwidth or observation time can reduce TDOA variances.

The maximum-likelihood (ML) estimator is efficient and is asymptotically normal with covariance matrix given by the CRLB [11]. Using ML estimation for

TABLE I
Computation of MSE Geometric Factor

$t = (x^o, y^o, z^o)$	
$s_i = (x_i, y_i, z_i)$	$i = 1, 2, 3$
$\rho_i = \dfrac{s_i - t}{\|s_i - t\|}$	$i = 1, 2, 3$
$\theta_{i,j} = \cos^{-1}\rho_i \cdot \rho_j$	$j < i \quad , \quad i = 1, 2, 3$
$\phi_i = \cos^{-1}\dfrac{t \cdot \rho_i}{\|t\|}$	$i = 1, 2, 3$
$\psi_i = \cos^{-1}\dfrac{\cos\phi_i - \cos\phi_{i+1}}{2\sin(\theta_{i+1,i}/2)}$	$i = 1, 2$
$w_i = \left\{2\sin\left(\dfrac{\theta_{i+1,i}}{2}\right)\sin\psi_i\right\}^{-1}$	$i = 1, 2$
$\alpha = \cos^{-1}\dfrac{\cos(\theta_{3,1}/2) - \cos\psi_1\cos\psi_2}{\sin\psi_1\sin\psi_2}$	
$G_e^2 = \dfrac{1}{\sin^2\alpha}(w_1^2 + w_2^2 + \cos\alpha\, w_1 w_2)$	

TDOAs, the joint pdf of $D_{2,1}$ and $D_{3,2}$ is

$$f(\Delta D_{2,1}, \Delta D_{3,2}) = \frac{1}{2\pi|Q|^{1/2}}\exp\left\{-\tfrac{1}{2}[\Delta D_{2,1}\ \Delta D_{3,2}]Q^{-1}\begin{bmatrix}\Delta D_{2,1}\\ \Delta D_{3,2}\end{bmatrix}\right\}$$

$$Q = \begin{bmatrix}\sigma_D^2 & -\sigma_D^2/2\\ -\sigma_D^2/2 & \sigma_D^2\end{bmatrix}. \qquad (29)$$

Hence

$$\Pr(\Delta D_{2,1}\,\Delta D_{3,2} < 0) = \tfrac{2}{3},$$

$$E[|\Delta D_{2,1}\,\Delta D_{3,2}| \mid \Delta D_{2,1}\Delta D_{3,2} < 0] = 0.91350\sigma_D^2$$

and

$$\Pr(\Delta D_{2,1}\,\Delta D_{3,2} > 0) = \tfrac{1}{3},$$

$$E[|\Delta D_{2,1}\,\Delta D_{3,2}| \mid \Delta D_{2,1}\Delta D_{3,2} > 0] = 0.32700\sigma_D^2. \qquad (30)$$

For $\sigma_p^2 = 0$, which is valid if all satellite positions are known exactly, then according to (22)–(27), the minimum MSE can be simplified to

$$\mathrm{MSE}_{\min} = G_e^2(c\sigma_D)^2$$

$$G_e^2 = \frac{1}{\sin^2\alpha}\{w_1^2 + w_2^2 + \cos\alpha w_1 w_2\} \qquad (31)$$

where G_e is the geometric factor dependent on the localization geometry. For clarity, the steps for computing G_e are summarized in Table I. Hahn and

Tretter's [10] TDOA estimator is an implementation of the ML estimator and can attain the CRLB. Thus optimum performance can be achieved by using their TDOA estimator.

The geometric factor G_e deserves much attention. It acts as a multiplicative factor to the TDOA variance to form the minimum MSE. The localization accuracy varies with G_e. We investigate the geometric factor in detail through simulations. In fact, for a given satellite spacing, there is a lower bound on G_e, regardless of the location geometry. Additionally, there is another lower bound on G_e, regardless of satellite spacing and location geometry.

We can observe from (19) that the error vectors on Earth are greater than the free-space error vectors by a factor of $1/\sin\psi_i$. The lower bound of MSE is obtained by setting ψ_i equal to unity. In such a case, we have $\alpha = \theta_{3,1}/2$ from (26) and $w_i = \{2\sin(\theta_{i+1,i}/2)\}^{-1}$, $i = 1,2$ from (24). Hence according to (31)

$$G_e^2 > TH = \frac{1}{4\sin^2(\theta_{3,1}/2)} \times \left\{ \frac{1}{\sin^2(\theta_{2,1}/2)} + \frac{1}{\sin^2(\theta_{3,2}/2)} + \frac{\cos(\theta_{3,1}/2)}{\sin(\theta_{2,1}/2)\sin(\theta_{3,2}/2)} \right\}. \quad (32)$$

Notice that all the terms on the right are positive. With a fixed $\theta_{3,1}$ and the approximation $\theta_{3,1} \approx \theta_{2,1} + \theta_{3,2}$ (this is valid since $r_s \gg r_E$), it can be easily shown that the minimum value of TH is

$$TH = \frac{1}{2\sin^2(\theta_{3,1}/2)} \left\{ \frac{3}{1-\cos(\theta_{3,1}/2)} - 1 \right\} \quad (33)$$

when $\theta_{2,1} = \theta_{3,2} = \theta_{3,1}/2$. Thus if $\sigma_{D21}^2 = \sigma_{D32}^2$, equal satellite separation can give a better result.

Keeping receiver positions fixed, $\theta_{3,1}$ attains its maximum value when the transmitter is on the equator and at the middle of s_1 and s_3. If the angle between s_1 and s_3 measured from the Earth center is η, simple geometry shows that they are related by $r_E/\sin(\theta_{3,1}/2 - \eta/2) = r_s/\sin(\theta_{3,1}/2)$. Hence

$$\frac{\theta_{3,1}}{2} = \tan^{-1}\frac{r_s\sin(\eta/2)}{r_s\cos(\eta/2) - r_E}. \quad (34)$$

Using (33) together with (34), the bound as a function of satellite span between s_1 and s_3 can be computed. This is useful in system design because it gives the limiting performance for a particular angle of satellite span.

Appendix A shows that the maximum value of $\theta_{3,1}$ is 180°. According to (33), the lower bound is $G_e > 1$ for all possible localization geometry. In other words, the localization uncertainty cannot be smaller than that of transmission path differences.

C. Bias in Transmitter Location

Transmitter position (x,y,z) are nonlinearly related to the random variables $D_{2,1}$ and $D_{3,2}$ and thus there is a bias in the position estimate. It is not an easy task to find the bias directly from the TDOA equations (2). The exact solution in Section II allows us to find an explicit solution of transmitter position in terms of the TDOAs, giving a simple way to compute the bias. Let the expected values of $D_{2,1}$ and $D_{3,2}$ be, respectively, $D_{2,1}^0$ and $D_{3,2}^0$. To find bias, we take a Taylor series expansion of the solution around $(D_{2,1}^0, D_{3,2}^0)$ and retain up to second-order terms. For the x coordinate, we have

$$\begin{aligned} x(D_{2,1}, D_{3,2}) = {} & x(D_{2,1}^0, D_{3,2}^0) + \frac{\partial x(D_{2,1}^0, D_{3,2}^0)}{\partial(cD_{2,1})} c\Delta D_{2,1} \\ & + \frac{\partial x(D_{2,1}^0, D_{3,2}^0)}{\partial(cD_{3,2})} c\Delta D_{3,2} \\ & + \frac{1}{2}\frac{\partial^2 x(D_{2,1}^0, D_{3,2}^0)}{\partial(cD_{2,1})^2}(c\Delta D_{2,1})^2 \\ & + \frac{1}{2}\frac{\partial^2 x(D_{2,1}^0, D_{3,2}^0)}{\partial(cD_{3,2})^2}(c\Delta D_{3,2})^2 \\ & + \frac{\partial^2 x(D_{2,1}^0, D_{3,2}^0)}{\partial(cD_{2,1})(cD_{3,2})}(c\Delta D_{2,1})(c\Delta D_{3,2}). \end{aligned} \quad (35)$$

The truncation error is small when $(D_{2,1}, D_{3,2})$ is close to $(D_{2,1}^0, D_{3,2}^0)$. Taking expectation of (35) and using (28), the minimum bias in the x direction is

$$\begin{aligned} b_x &= K_x(c\sigma_D)^2 \\ K_x &= \frac{1}{2}\left\{ \frac{\partial^2 x(D_{2,1}^0, D_{3,2}^2)}{\partial(cD_{2,1})^2} + \frac{\partial^2 x(D_{2,1}^0, D_{3,2}^2)}{\partial(cD_{3,2})^2} - \frac{\partial^2 x(D_{2,1}^0, D_{3,2}^2)}{\partial(cD_{2,1})(cD_{3,2})} \right\}. \end{aligned} \quad (36)$$

Similarly,

$$b_y = K_y(c\sigma_D)^2 \quad \text{and} \quad b_z = K_z(c\sigma_D)^2 \quad (37)$$

where K_y and K_z are defined analogous to K_x in (36) with x replaced by y and z, respectively. We define the total bias as

$$b = G_b(c\sigma_D)^2, \qquad G_b = \sqrt{K_x^2 + K_y^2 + K_z^2} \quad (38)$$

where G_b is termed as the geometric factor for bias, as it is dependent on the geometric configuration only.

Let us compare the bias squared and MSE. Their ratio is given by

$$\frac{b^2}{\text{MSE}} = \frac{G_b^2}{G_e}(c\sigma_D)^2 \quad (39)$$

which is proportional to the variance of TDOA. If $c^2\sigma_D^2$ is small, the bias is insignificant compared with MSE.

Although in the preceding study we assume the two TDOAs to have equal variances, the results can be easily generalized to unequal variances. In such a case, the contributions of w_1 and w_2 to the geometric factor G_e in (31) are proportional to their corresponding TDOA variances. Choosing satellite separations $\theta_{2,1}$ and $\theta_{3,2}$ inversely proportional to their respective TDOA variances can achieve a better performance and the contribution to bias of the two TDOA curves will be different.

IV. SIMULATION RESULTS

In the following, we assume that the transmitter is on Earth and the three geostationary satellites are equally spaced. That is, the distances between s_1 and s_2, and s_2 and s_3 are identical. We take satellite spacing as the angle between s_i and s_{i+1} measured from the Earth center. For simplicity, we consider an ideal situation where the latitudes of satellites are zero, i.e., their z coordinate is zero. In this case, the matrix in (7) becomes singular. By subtracting the second row from the first and third rows, it can be expressed as

$$\begin{bmatrix} x_1 - x_2 & y_1 - y_2 \\ x_3 - x_2 & y_3 - y_2 \end{bmatrix} \begin{bmatrix} x \\ y \end{bmatrix} = \frac{1}{2} \begin{bmatrix} K_1 - K_2 + r_{2,1}^2 + 2r_{2,1}r_2 \\ K_3 - K_2 - r_{3,2}^2 - 2r_{3,2}r_2 \end{bmatrix} \tag{40}$$

and x and y can then be solved in terms of r_2. Substitution of this result into (5) with $i = 2$ gives a quadratic equation in r_2. Inserting the positive root to (40) yields a unique x and y solution. The unit of distance is kilometer. Hence the bias geometric factor has a unit of 1/km.

In the first simulation, we fix the transmitter position and determine how the geometric factors of MSE and bias are affected by satellite spacing. The transmitter position is at 45.35°N and 75.9°W, which is the location of Ottawa, Canada. Receiver s_2 is fixed at 70°W longitude and the satellite separation is adjusted by changing the positions of s_1 and s_3. The measured TDOAs are simulated by adding zero mean correlated Gaussian noises ε_1 and ε_2 to the true values with their correlation matrix set according to Q in (29). σ_D^2 is set to $0.001/c^2$. For each TDOA pairs $D_{2,1}$ and $D_{3,2}$, the transmitter positions are computed from (40) and position errors squared are averaged to form the MSE. After normalizing with $c^2\sigma_D^2$, the results are plotted in Fig. 5(a). As expected, when the separation increases, the geometric factor decreases rapidly. For example, with 5° separation, G_e is 251. When the separation is increased to 30°, it drops to 7.1. Following the steps in Table I, the predicted change in G_e with respect to satellite spacing is also given in Fig. 5(a). The two

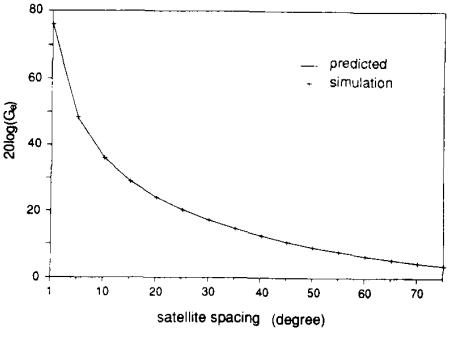

(a)

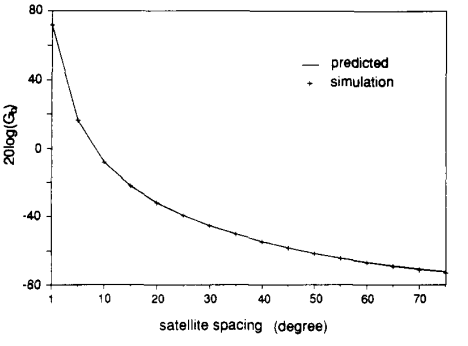

(b)

Fig. 5. Variation of geometric factors with satellite spacing. (a) MSE geometric factor. (b) Bias geometric factor.

curves are in close match. Validity of the formula in (31) is confirmed.

With the same transmitter location, Fig. 5(b) shows the dependency of bias on satellite spacing. One is computed by using the derived formula (38) while the other is obtained by simulations under the same conditions as before. They are both normalized by $c^2\sigma_D^2$. Due to limited space, we only show the total bias geometric factor G_b in the figure. In fact, K_x, K_y, and K_z are all negative. Moreover, $|K_z| \gg |K_x| > |K_y|$. That means, for receivers in geostationary orbits, bias in z direction is most dominant and $G_b \approx |K_z|$. As observed in Fig. 5(b), simulated and predicted results coincide with each other and the correctness of (38) is corroborated. The bias decreases as satellite separation increases. Comparing with Fig. 5(a), the bias geometric factor follows the same trend as the MSE geometric factor but decreases at a rate double the other. At large separation, the bias is small enough to be neglected.

To corroborate the bound on G_e as a function of satellite span, we plot (33) together with (34) in Fig. 6. In our configuration, $\eta/2$ is equal to the satellite spacing. It is compared with the simulation results from searching for the smallest possible MSE by varying transmitter position for a particular satellite

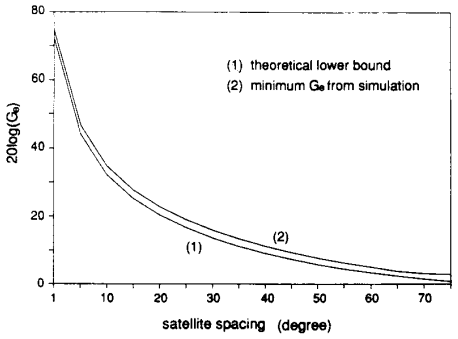

Fig. 6. Comparison of theoretical lower bound with simulation results on MSE geometric factor with respect to satellite spacings.

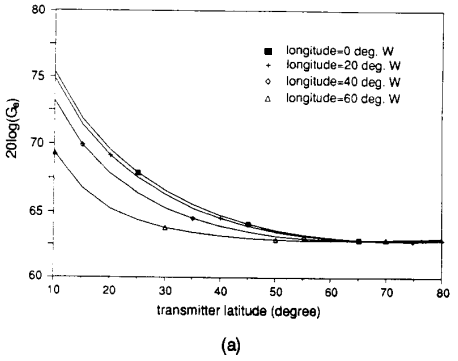

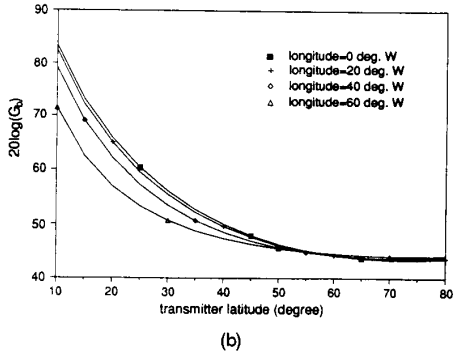

Fig. 7. Simulated results on variations of geometric factors on transmitter location. Satellite separation is 2°. (a) MSE geometric factor. (b) Bias geometric factor.

separation. As seen from Fig. 6, the bound is only lower than the true value by a factor of about 1.34.

We next investigate how the transmitter location affects the localization accuracy. Two cases are studied, one for closely spaced satellites at 2° separation and the other at a large separation of 30°. The first situation corresponds to satellite interference location because transmitter beamwidth is usually small, while the other corresponds to SARSAT localization as the transmitter antenna gain is

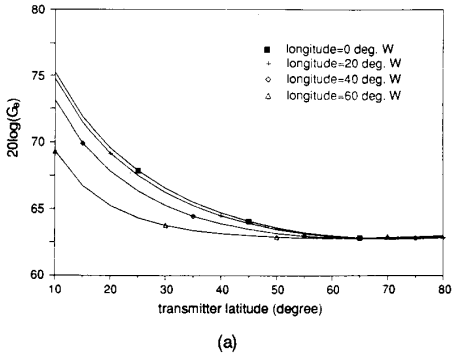

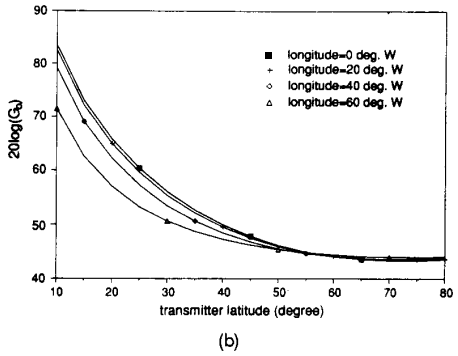

Fig. 8. Predicted variations of geometric factors on transmitter location. Satellite separation is 2°. (a) MSE geometric factor. (b) Bias geometric factor.

small to allow a large beamwidth. The satellite s_2 is fixed at 0° longitude. The simulated results for the two cases are given in Fig. 7 and Fig. 9. The predicted accuracies are given in Fig. 8 and Fig. 10, respectively. Only the results for positive latitude and longitude were shown because same curves were obtained for negative longitude or latitude due to symmetry. We can see from the Figures that the predicted and simulated geometric factors of MSE and bias are almost identical. These results again corroborate the validity of the theoretical developments.

It is clear in Fig. 7 or Fig. 8 that as the transmitter latitude increases, both G_e and G_b decrease rapidly. At small latitude, increasing longitude can also decrease the geometric factors. Although we have not shown in the Figures, both G_e and G_b approach infinity at zero transmitter latitude, for the reason that the two hyperbolic curves intercept at very small angles and create a large uncertainty in position fixing. Notice that the values G_e and G_b are very large. This implies TDOA measurements need to be very accurate in order to get an acceptable transmitter location estimate. For example, to obtain a transmitter location at latitude greater than 40° with a root MSE of 2 km, we find from Fig. 7 that G_e should be smaller than

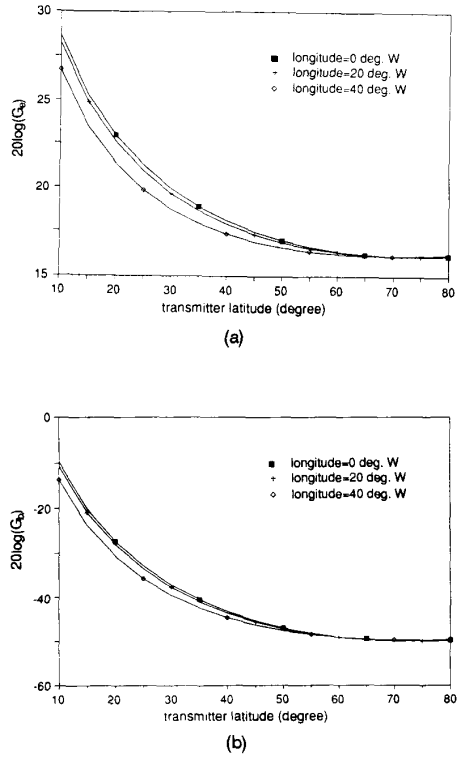

Fig. 9. Simulated results on variations of geometric factors on transmitter location. Satellite separation is 30°. (a) MSE geometric factor. (b) Bias geometric factor.

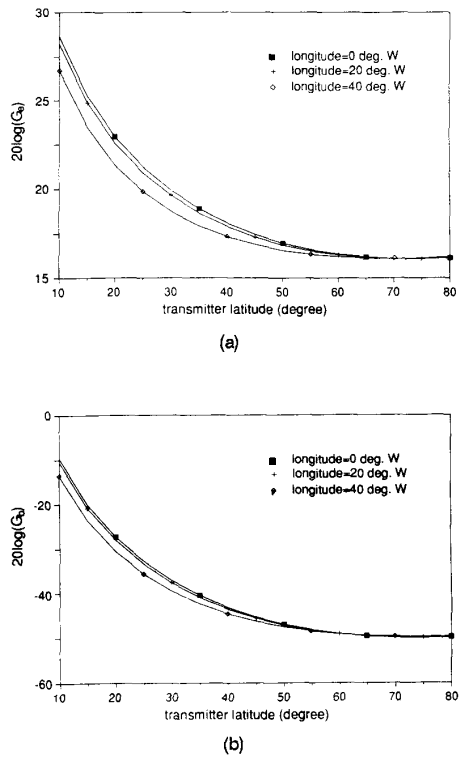

Fig. 10. Predicted variations of geometric factors on transmitter location. Satellite separation is 30°. (a) MSE geometric factor. (b) Bias geometric factor.

1718. According to (31) the TDOA standard deviation must be less than 3.88 ns.

In the case of large satellite separation, observations are similar: both G_e and G_b decrease in the same pattern as in the previous case. There is, however, a significant gain in the reduction of geometric factors. In the above example with 2 km localization accuracy, a TDOA standard deviation of 0.832 μs is sufficient for satellite separation of 30°.

V. CONCLUSION

Geolocation of a transmitter from TDOAs measured by three or four geostationary satellites were studied and analyzed. A noniterative method to solve for a transmitter location from the measurement equations was proposed. Expressions for localization MSE and bias were derived, as were the CRLB in localization accuracy and the relationship between MSE and satellite span. When ignoring satellite position uncertainties, the MSE and bias can be expressed as a product of differential distance variance $c^2\sigma_D^2$ and a factor that is dependent on localization geometry. The geometric factors of MSE and bias decrease as satellite spacing, transmitter latitude or transmitter longitude increases. Theoretical solutions were corroborated by simulation results.

A drawback for the system is that when the transmitter has a narrow beamwidth, the separation between satellites are restricted to be small. Consequently, the angle of intersection of the two hyperbolic curves on Earth are so small that it gives large geometric factors. The TDOAs must be very accurate in order to obtain an acceptable solution. The accuracy can be improved substantially if the antenna beamwidth of the transmitter is large to allow for a greater satellite separation.

APPENDIX A

There is a limit on the TDOA of a signal received by geostationary satellites. As shown in Fig. 11, maximum path difference occurs when the two satellites s_1 and s_2 are η apart and the transmitter t is on the equator with the same longitude as s_1. The angle η is such that $\delta = 90°$, since electromagnetic wave can only travel in straight line. With the Earth radius r_E equal to 6378 km and the geostationary orbit

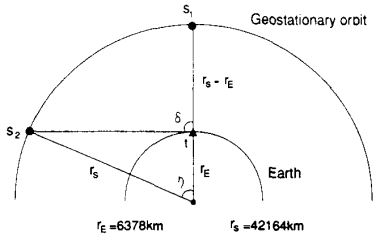

Fig. 11. Geolocation geometry for maximum TDOA.

radius r_s given by 42164 km, we have

$$\eta = \cos^{-1}\frac{r_E}{r_s} \approx 81.3°. \tag{41}$$

Hence

$$\text{TDOA}_{\max} = \frac{ts_2 - ts_1}{c} = 19.64 \text{ ms} \tag{42}$$

where $c = 3 \times 10^5$ km/s is the signal propagation speed. The maximum geostationary satellite span is, of course, equal to $2\eta = 162.6°$ when measured from the Earth center.

APPENDIX B

The gradient vectors for the two hyperbolae are given by [8]

$$\nabla \mathbf{r}_{2,1} = (\rho_1 - \rho_2), \qquad \nabla \mathbf{r}_{3,2} = (\rho_2 - \rho_3). \tag{43}$$

Their dot product is

$$\nabla \mathbf{r}_{2,1} \cdot \nabla \mathbf{r}_{3,2} = \cos\theta_{2,1} + \cos\theta_{3,2} - \cos\theta_{3,1} - 1. \tag{44}$$

When the three receivers are on a geostationary orbit, we have $\theta_{3,1} \approx \theta_{2,1} + \theta_{3,2}$ because r_E is much less than r_s. Using trigonometric identities, (44) can then be rewritten as

$$\begin{aligned}\nabla \mathbf{r}_{2,1} \cdot \nabla \mathbf{r}_{3,2} &= 2\cos\frac{\theta_{2,1}+\theta_{3,2}}{2}\cos\frac{\theta_{2,1}-\theta_{3,2}}{2} - 2\cos^2\frac{\theta_{3,1}}{2} \\ &= 4\cos\frac{\theta_{3,1}}{2}\sin\frac{\theta_{2,1}}{2}\sin\frac{\theta_{3,2}}{2}.\end{aligned} \tag{45}$$

It is evident that the angle between the two gradient vectors is less than 90°, since $\theta_{3,1}$ is smaller than 180°. In fact, according to (43) the magnitudes of the two gradient vectors are

$$|\nabla \mathbf{r}_{2,1}| = 2\sin(\theta_{2,1}/2), \qquad |\nabla \mathbf{r}_{3,2}| = 2\sin(\theta_{3,2}/2) \tag{46}$$

and therefore the angle ζ between them is simply equal to

$$\zeta = \frac{\theta_{3,1}}{2}. \tag{47}$$

APPENDIX C

It is obvious that α is the angle between vectors $\mathbf{v}_1$ and $\mathbf{v}_2$, where $\mathbf{v}_i$ are the projections of $\nabla \mathbf{r}_{i+1,i}$ onto the Earth surface, $i = 1,2$. Since they must be perpendicular to $\mathbf{r}$, we have

$$\begin{aligned}\mathbf{v}_i &= \nabla \mathbf{r}_{i+1,i} - (\mathbf{r}^T \nabla \mathbf{r}_{i+1,i})\mathbf{r} \\ &= \rho_i - \rho_{i+1} - (\cos\phi_i - \cos\phi_{i+1})\mathbf{r}, \\ & \qquad i = 1,2.\end{aligned} \tag{48}$$

Hence using (45),

$$\begin{aligned}\mathbf{v}_1 \cdot \mathbf{v}_2 = 4\cos\frac{\theta_{3,1}}{2}\sin\frac{\theta_{2,1}}{2}\sin\frac{\theta_{3,2}}{2} \\ - (\cos\phi_1 - \cos\phi_2)(\cos\phi_2 - \cos\phi_3)\end{aligned} \tag{49}$$

and using (46),

$$\begin{aligned}\|v_i\|^2 = 4\sin^2\frac{\theta_{i+1,i}}{2} - (\cos\phi_i - \cos\phi_{i+1})^2, \\ i = 1,2.\end{aligned} \tag{50}$$

Hence

$$\begin{aligned}\cos\alpha &= \frac{\mathbf{v}_1 \cdot \mathbf{v}_2}{\|\mathbf{v}_1\|\|\mathbf{v}_2\|} \\ &= \frac{\cos(\theta_{3,1}/2) - \cos\psi_1\cos\psi_2}{\sin\psi_1\sin\psi_2}\end{aligned} \tag{51}$$

where [8]

$$\psi_i = \cos^{-1}\frac{\cos\phi_i - \cos\phi_{i+1}}{2\sin(\theta_{i+1,i}/2)}, \qquad i = 1,2. \tag{52}$$

APPENDIX D

For simplicity, assume that the longitude of the transmitter is zero. Denote the transmitter latitude by *lat*. After taking partial derivatives of z with respect to x and y, the plane which is tangent to Earth at a transmitter location is

$$z = -\cot(\text{lat})x + r_E\{\sin(\text{lat}) + \cot(\text{lat})\cos(\text{lat})\}. \tag{53}$$

The signal from the emitter can only be radiated in the region above this plane. The intersection of this plane with the equatorial plane gives two critical satellite positions that can still receive the signal. By setting $z = 0$ in (D1), the x coordinate of the satellite is

$$x_c = r_E\{\sin(\text{lat})\tan(\text{lat}) + \cos(\text{lat})\}. \tag{54}$$

The maximum angle of satellite separation is therefore

$$2\tan^{-1}\frac{\sqrt{r_s^2 - x_c^2}}{x_c}. \tag{55}$$

REFERENCES

[1] Scales, W. C., and Swanson, R. (1984) Air and sea rescue via satellite systems. *IEEE Spectrum* (Mar. 1984), 48–52.

[2] Smith, W. W., and Steffes, P. G. (1989)
Time-delay techniques for satellite interference location system.
IEEE Transactions on Aerospace and Electronic Systems, **25**, 2 (Mar. 1989), 224–230.

[3] Ha, T. T., and Robertson, R. C. (1987)
Geostationary satellite navigation systems.
IEEE Transactions on Aerospace and Electronic Systems, **AES-23**, 2 (Mar. 1987), 247–254.

[4] Sonnenschein, A., and Hutchinson, W. K. (1990)
Geolocation of frequency-hopping transmitters via satellites.
IEEE MILCOM, Monterey, CA, 1990, 297–303.

[5] Foy, W. H. (1976)
Position-location solutions by Taylor series estimation.
IEEE Transactions on Aerospace and Electronic Systems, **AES-12**, 2 (Mar. 1976), 187–194.

[6] Torrieri, D. J. (1984)
Statistical theory of passive location systems.
IEEE Transactions on Aerospace and Electronic Systems, **AES-20**, 2 (Mar. 1984), 183–198.

[7] Fang, B. T. (1990)
Simple solutions for hyperbolic and related position fixes.
IEEE Transactions on Aerospace and Electronic Systems, **26**, 5 (Sept. 1990), 748–753.

[8] Chestnut, P. C. (1982)
Emitter location accuracy using TDOA and differential doppler.
IEEE Transactions on Aerospace and Electronic Systems, **AES-18**, 2 (Mar. 1982), 214–218.

[9] Knapp, C. H., and Carter, G. C. (1976)
The generalized correlation method for estimation of time delay.
IEEE Transactions on Acoustics, Speech, Signal Processing, **ASSP-24**, 4 (Aug. 1976), 320–327.

[10] Hahn, W. R., and Tretter, S. A. (1973)
Optimum processing for delay-vector estimation in passive signal arrays.
IEEE Transactions on Information Theory, **IT-19**, 5 (Sept. 1973), 608–614.

K. C. Ho (S'89—M'91) was born in Hong Kong on July 28, 1965. He received the B.Sc. degree with First Class Honours in Electronics and the Ph.D. degree in Electronic Engineering from the Chinese University of Hong Kong, Hong Kong, in 1988 and 1991, respectively. He was the recipient of the Croucher Foundation Studentship from 1988 to 1991.

He is currently a Research Associate at the Department of Electrical and Computer Engineering, Royal Military College of Canada, Kingston, Ontario. His research interests are in digital signal processing, source localization, and developing efficient adaptive algorithms for various applications including time delay estimation, noise cancellation and system identification.

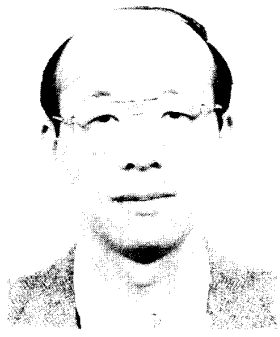

Y. T. Chan (SM'80) was born in Hong Kong. He received the B.Sc. and M.Sc. degrees from Queen's University, Kingston, Ontario, Canada, in 1963 and 1967, and the Ph.D. degree from the University of New Brunswick, Fredericton, Canada, in 1973, all in electrical engineering.

He has worked with Northern Telecom Ltd. and Bell-Northern Research. Since 1973 he has been at the Royal Military College of Canada, Kingston, Ontario, where he is presently a Professor. He has served as a consultant on sonar systems. His research interests are in sonar signal processing and passive localization and tracking techniques.

Dr. Chan was an Associate Editor (1980–1982) of the *IEEE Transactions on Signal Processing* and was the Technical Program Chairman of the 1984 International Conference on Acoustics, Speech and Signal Processing (ICASSP'84). He directed a NATO Advanced Study Institute on Underwater Acoustic Data Processing in 1988 and was the General Chairman of ICASSP'91 held in Toronto, Canada.